CHEMISTRY
A EUROPEAN JOURNAL

DOI: 10.1002/chem.200500840

In Search of Ionic Liquids Incorporating Azolate Anions

Alan R. Katritzky,*[a] Shailendra Singh,[a] Kostyantyn Kirichenko,[a] Marcin Smiglak,[b] John D. Holbrey,*[b, c] W. Matthew Reichert,[b] Scott K. Spear,[b] and Robin D. Rogers*[b]

Abstract: Twenty-eight novel salts with tetramethyl-, tetraethyl-, and tetrabutylammonium and 1-butyl-3-methylimidazolium cations paired with 3,5-dinitro-1,2,4-triazolate, 4-nitro-1,2,3-triazolate, 2,4-dinitroimidazolate, 4,5-dinitroimidazolate, 4,5-dicyanoimidazolate, 4-nitroimidazolate, and tetrazolate anions have been prepared and characterized by using differential scanning calorimetry (DSC), thermogravimetric analysis (TGA), and single-crystal X-ray crystallography. The effects of cation and anion type and structure on the physicochemical properties of the resulting salts, including several ionic liquids, have been examined and discussed. Ionic liquids (defined as having m.p. $< 100\,^{\circ}C$) were obtained with all combinations of the 1-butyl-3-methylimidazolium cation ($[C_4mim]^+$) and the heterocyclic azolate anions studied, and with several combinations of tetraethyl or tetrabutylammonium cations and the azolate anions. The $[C_4mim]^+$ azolates were liquid at room temperature exhibiting large liquid ranges and forming glasses on cooling with glass-transition temperatures in the range of -53 to $-82\,^{\circ}C$ (except for the 3,5-dinitro-1,2,4-triazolate salt with m.p. $33\,^{\circ}C$). Six crystal structures of the corresponding tetraalkylammonium salts were determined and the effects of changes to the cations and anions on the packing of the structure have been investigated.

Keywords: azolates · crystal structures · imidazolium salts · ionic liquids · phase transitions

Introduction

The growing social pressure for new green technologies and the promise of ionic liquids (ILs) to deliver such has led to high academic and industrial interest in IL technologies.[1–10] Ionic liquids make a unique architectural platform on which, at least potentially, the properties of both anion and cation components can be independently modified, enabling tunability in the design of new functional materials. This design approach can be used as a platform strategy to deliver different functional attributes in the corresponding cationic and anionic components of an IL, while retaining the core desirable features of the IL state of matter, and has applicability in many different materials areas.

The desire to develop energetic salts[11] as advanced materials with reduced environmental footprints and overall exposure to hazardous and potentially toxic materials including hydrazine, metals, and perchlorates, has led to renewed efforts to explore this area. Drake and co-workers utilized one aspect of the platform approach to IL design to prepare nonvolatile, thermally stable, liquid energetic materials[12] by combining energetic cations (based on 1,2,4-triazole, 4-amino-1,2,4-triazole, and 1,2,3-triazole cores[13]) and anions ($[NO_3]^-$, $[ClO_4]^-$, and $[N(NO_2)_2]^-$). It was suggested that the ready formation of ILs using these cations was due to their similar topographical shape and charge distribution to more conventional imidazolium cations.

Our interest in functionalized heterocycles in this context comes from 1) the ongoing study of the formation of ILs

[a] Prof. A. R. Katritzky, Dr. S. Singh, Dr. K. Kirichenko
Center for Heterocyclic Compounds
University of Florida
Department of Chemistry
Gainesville, FL 32611-7200 (USA)
Fax: (+1) 352-392-9199
E-mail: Katritzky@chem.ufl.edu

[b] M. Smiglak, Dr. J. D. Holbrey, Dr. W. M. Reichert, Dr. S. K. Spear, Prof. R. D. Rogers
Center for Green Manufacturing and Department of Chemistry
The University of Alabama
Tuscaloosa, AL 35487 (USA)
Fax: (+1) 205-348-0823
E-mail: j.holbrey@qub.ac.uk
RDRogers@bama.ua.edu

[c] Dr. J. D. Holbrey
Current address: The QUILL Research Centre
Queen's University of Belfast
BT9 5AG, Northern Ireland (UK)

Supporting information for this article (showing the chemical structures of the azolate salts explored for IL behavior) is available on the WWW under http://www.chemeurj.org/ or from the author.

containing energetic components, in which heterocycles can furnish either the cationic or anionic portion of the resultant salt, and 2) investigation of the influence of heterocycle substitution patterns on the ability of these materials to form IL phases. That is, using the platform strategy to deliver the energetic characteristics of nitro- and amine-substituted heterocycles in an IL material in which the liquid characteristics are controlled through the complementary counterion.

Whereas nitro- and cyano-functionalized imidazoles can be used to prepare imidazolium-based ILs,[14] the addition of electron-withdrawing substituents leads to an overall destabilization of the heterocyclic cation relative to the corresponding azole, thus limiting their applicability in the formation of conventional ILs. However, the anionic azolate form of the heterocycles are stabilized further by the introduction of such electron-withdrawing substituents and presents opportunities to investigate the formation of ILs containing heterocyclic anions.

Surprisingly, the investigation of potential ILs containing planar heterocyclic anions has been largely neglected. A small number of tetraalkylammonium and -phosphonium 1,2,4-triazolates and imidazolates (formed from onium halides and azolates) have been described as solvents and highly active catalysts for oligomerization of isocyanates in the patent literature.[15] Ohno et al. described the preparation and electrochemical properties of two ILs 1-ethyl-3-methylimidazolium tetrazolate and triazolate, which were prepared through the reaction of imidazolium hydroxide (generated by anion exchange from the halide) with the corresponding azole.[16,17]

This formation of low-melting, relatively low-viscosity ILs containing both heterocyclic planar cations and anions was somewhat unexpected and prompted us to investigate whether comparable low-melting ILs could be prepared incorporating highly functionalized azolate anions. The salt, tetrabutylammonium 4-nitroimidazolate[18] (m.p. 120 °C), had been reported as an intermediate for the synthesis of *N*-alkyl-4-nitroimidazoles, and following this, we described the formation of 1-butyl-3-methylimidazolium 3,5-dinitro-1,2,4-triazolate, a crystalline low-melting solid (m.p. ≈33 °C), which demonstrated that ILs could be readily obtained even with more highly functionalized heterocyclic anions[19] by using the appropriate selection of complementary cations and anions.

Most recently, Shreeve and co-workers[20,21] have reported that a wide range of energetic azolium azolate salts can be prepared with melting points approaching the definition of "ionic liquids", however to date, a systematic study of the complementarity of cation and anion selection, which can be used to obtain room-temperature energetic ILs, has not been reported.

To extend the scope of these promising results, the availability of more organic anions (rather than the common inorganic anions now in vogue) that provide the same architectural flexibility as the commonly used organic cations currently studied (e.g., substituted imidazolium cations) needs to be achieved. With diverse anions available, an improvement in the basic understanding of the key physical and chemical properties of these complex liquids can be made.

Here we present the synthesis and characterization, including elucidation of solid-state crystal structures, of a systematic series of twenty-eight novel tetraalkylammonium and 1-butyl-3-methylimidazolium ($[C_4mim]^+$) salts prepared by combining the four cations with seven heterocyclic tetrazolate, triazolate, and imidazolate anions. Figure 1 illustrates

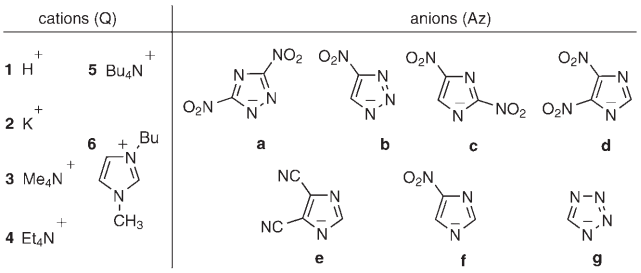

Figure 1. Cations and anions explored in this work (note: compounds **1a**–**g** are covalent, all others are ionic salts).

the diversity of azolate salts that can be prepared by using simple procedures (also see Figure 1 in the Supporting Information). Many of the azoles used to furnish the anion component of these salts are energetic heterocyclic compounds and have been studied extensively as potential energetic materials. The ability to readily form IL examples with enhanced stability relative to the starting heterocycles (controlling melting points, higher thermal decomposition temperature, and reduced volatility), and the generic observation that IL materials can be formed from a wide range of flat heterocyclic anions by modification or selection of the appropriate ions, sets out principles by which ILs containing a new class of anions can be developed and exploited.

Results and Discussion

Organic tetraalkylammonium (methyl, ethyl, butyl) and 1-butyl-3-methylimidazolium salts were prepared with seven different azolate anions (Figure 1), 3,5-dinitro-1,2,4-triazolate (**a**), 4-nitro-1,2,3-triazolate (**b**), 2,4-dinitroimidazolate (**c**), 4,5-dinitroimidazolate (**d**), 4,5-dicyanoimidazolate (**e**), 4-nitroimidazolate (**f**), and tetrazolate (**g**), by metathesis reaction of the corresponding potassium azolate salts with the tetraalkylammonium or $[C_4mim]^+$ halides in acetone/dichloromethane. The cation choice was made in order to establish the broad relative potentials of the organic azolate salts prepared to form IL phases, using the progression in size from tetramethylammonium to tetrabutylammonium to identify the range of melting points that might be anticipated when using other cations that have a higher tendency to form IL salts, and to isolate crystalline salts from which solid-state data could be obtained by using X-ray crystallography analysis. Salts with $[C_4mim]^+$ cations were then prepared and examined to determine the validity of these pre-

dictions. ($[C_4mim]^+$ is currently the most investigated common IL supporting cation and it was used to give thermal data directly comparable to the body of existing IL systems.)

The potassium azolate salts **2a–d** were initially prepared by treatment of the corresponding azoles **1a–d** with potassium carbonate in acetone (Scheme 1). Reaction of potassium

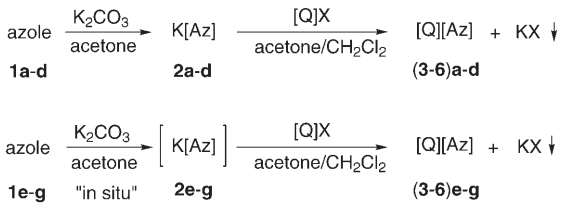

Scheme 1. Synthesis strategies.

azolates **2a–d** with equivalent amounts of appropriate tetraalkylammonium chlorides or bromides or $[C_4mim]^+$ chloride in acetone/dichloromethane (1:1 v/v) at 20–25 °C gave the corresponding tetraalkylammonium and $[C_4mim]^+$ azolates (**3–6**)**a–d** in high yields (78–99 %) after removal of the precipitated potassium halide and evaporation of the solvent.

It proved difficult to isolate pure potassium 4,5-dicyanoimidazolate (**2e**), potassium 4-nitroimidazolate (**2f**), and potassium tetrazolate (**2g**) due to their low solubility. For the synthesis of the organic 4,5-dicyanoimidazolate (**3–6**)**e**, 4-nitroimidazolate (**3–6**)**f**, and tetrazolate (**3–6**)**g** salts, the respective potassium azolate intermediates **2e–g** were generated in situ in the presence of potassium carbonate and not isolated. Thus, treatment of azoles **1e–g** with tetraalkylammonium or $[C_4mim]^+$ halides in the presence of potassium carbonate in acetone/dichloromethane gave good yields of ILs (**3–6**)**e–g** except salt **3g**, which was obtained in only 15 % yield, perhaps as a result of the low solubility of both tetramethylammonium chloride and potassium tetrazolate in acetone/dichloromethane.

The structures of salts (**3–6**)**a–g** were supported by data from ^1H and ^{13}C NMR spectra and elemental analyses (see the Experimental Section).

Thermal characterization: The salts varied in their physical state from high-melting-point solids (with tetramethylammonium cations) to ILs at room temperature, forming glassy solids on cooling ($[C_4mim]^+$ cations). The thermal behaviors of the salts (Table 1) were characterized by using differential scanning calorimetry (DSC). The crystalline salts all displayed a sharp melting transition on heating, and crystallized on cooling from the melt. However, in the bulk, several of the lower melting salts only crystallized very slowly on cooling from the melt. The melting transitions of many of the salts were poorly defined in the DSC data, commonly having a characteristic broad transition with a strong "leading edge". In contrast, the crystallization peaks were exceptionally sharp. This behavior has been observed for other IL-forming salts.[22]

The salts with the 3,5-dinitro-1,2,4-triazolate (**a**), 2,4-dinitroimidazolate (**c**), and 4-nitroimidazolate (**f**) anions all showed simple thermal behavior, with melting and crystallization or glass transitions (**6c** and **6f**) that were constant and independent of the sample's thermal history. The remaining salts, with 4-nitro-1,2,3-triazolate (**b**), 4,5-dinitroimidazolate (**d**), 4,5-dicyanoimidazolate (**e**), and tetrazolate (**g**) anions, showed more extensive and complicated behavior exhibiting both reversible solid–solid and irreversible transitions.

Salts (**3–4**)**a–g**, **5a–f**, and **6a** were crystalline or microcrystalline solids, which were isolated by precipitation from solution, whereas **5g** and all the $[C_4mim]^+$ cation salts **6b–g** were isolated as room-temperature liquids. The tetramethylammonium salts **3a–g** were high-melting solids with melting points ranging from 157 to 216 °C, with only small, or no liquid ranges and with decomposition generally being initiat-

Table 1. Thermal transitions for **3–6**(**a–g**) and related salts.[a]

	Me_4N^+ (**3**)		Et_4N^+ (**4**)		Bu_4N^+ (**5**)		$[C_4mim]^+$ (**6**)	
Anion	m.p.	T_{decomp}	m.p.	T_{decomp}	m.p.	T_{decomp}	m.p.	T_{decomp}
3,5-dinitro-1,2,4-triazolate (**a**)	214 (97)	235 (275)	114 (156)[c]	205 (296)	139 (186)	219 (298)	**33** (77)	239 (318)
4-nitro-1,2,3-triazolate (**b**)	157 (170)[b]	180	**82** (101)[c]	194	**87** (113)[c]	192	**−73**[d]	219
2,4-dinitroimidazolate (**c**)	181 (132)	222 (274)	**86** (132)	216 (271)	**81** (101)	221 (297)	**−53**[d]	254 (313)
4,5-dinitroimidazolate (**d**)	215[b]	225 (258)	**84** (97)	215 (253)	**85** (38)[c]	222 (287)	**−64**[d]	241 (288)
4,5-dicyanoimidazolate (**e**)	197[b]	202 (232)	118 (142)	212 (255)	**79** (85)[b]	215 (258)	**−74**[b]	230 (280)
4-nitroimidazolate (**f**)	185	165 (215)	124 (201)	188 (230)	106 (122)	193 (232)	**−63**[b]	200 (244)
tetrazolate (**g**)	216[b]	198 (241)	114 (138)[c]	189 (231)	**−66**[d]	180 (220)	**−82**[d]	208 (253)
bistriflimide	133[34]	–	109[34]	–	**96**[34]	–	**−86/−16/−5**[e][35,36]	–
triflate	>300[37]	–	160–161[38]	–	111–112[38]	–	**−82/3/16**[e][36]	–
tetrafluoroborate	>300	–	>300[39]	–	159–162	–	**−85–(−71)**[e][36,40]	–

[a] Melting (m.p.) or glass transition (T_g) points [°C] were measured from transition onset temperature and transition enthalpy ($J\,g^{-1}$, in parentheses) determined by using DSC from the second heating cycle at 5 °C min^{-1}, after initially melting and then cooling samples to −100 °C unless otherwise indicated. Decomposition temperatures (T_{decomp}) were determined by TGA, heating at 5 °C min^{-1} under argon, and are reported as onset to 5 wt % mass loss and are shown with the inflection point for total mass loss in parentheses. Salts meeting the definition of ionic liquids (m.p. < 100 °C) have values given in bold. [b] Reversible solid–solid transitions: **3b**, 118 (13); **3d**, 51 (7) and 86 (50); **3e**, 15 (14) and 60 (64); **3g**, 83 (82); **5e**, 52 (28). [c] Irreversible solid–solid transition, from first heating: **4a**, 102 (19); **4b**, 32 (83); **4g**, 49 (97); **5b**, 59 (16); **5d**, 55 (47). [d] Glass transitions, measured on cooling. [e] Glass transition/crystallization point/melting point.

ed upon melting. For each of the anions here, increased cation size is connected with a significant decrease in melting point. The tetraethylammonium salts **4a–g** all exhibited melting points around 100 °C (82–124 °C), which corresponded to a destabilization of the crystal state of around 100 °C relative to the tetramethylammonium analogues. When the larger tetrabutylammonium cation was used (**5a–g**), a greater variation in the melting point with anion was observed, from 139 °C for **5a** to room-temperature liquid with sub-ambient glass formation for **5g**. The characteristic heating and cooling profiles for the tetrabutylammonium salts **5a**,**c–f** are shown in Figure 2.

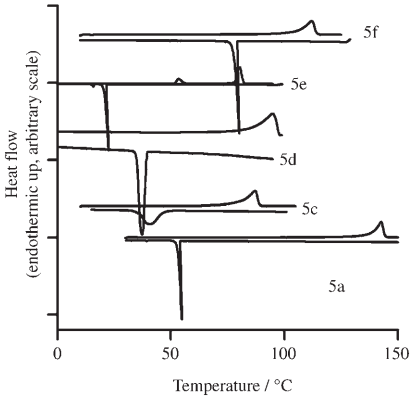

Figure 2. Characteristic DSC traces for the tetrabutylammonium salts **5a**,**c–f** showing the characteristic broad melting and sharp crystallization transitions, and the relative changes in melting point with anion type. Transitions are shown from the second heating and cooling cycles.

As anticipated, introduction of the asymmetric $[C_4mim]^+$ cation (**6**) led to a further reduction in the melting points of the salts. Salts **6b–g** were liquids at room temperature, and **6a**, the only $[C_4mim]^+$ salt isolated as a crystalline solid, had a melting point of only 33 °C. The ILs with $[C_4mim]^+$ cations **6b–g** showed only a glass transition point in the range between −53 and −82 °C, and no freezing transition was observed. This behavior, widely observed in IL samples, is comparable to the results reported for 1-ethyl-3-methylimidazolium triazolate and tetrazolate by Ohno and co-workers.[16]

In the 4,5-dinitroimidazolate (**d**) series, reversible solid–solid transitions were observed for **3d** at 51 and 86 °C. In contrast, **5d** showed a sharp solid–solid transition at 55 °C in the first heating cycle followed by a broad melting transition at ≈95 °C. On cooling, the sample of **5d** crystallized at 65 °C, and on subsequent heating scans, melted at 85 °C.

For the 4,5-dicyanoimidazolates (**e**), two reversible crystal–crystal transitions at 15 and 60 °C were observed for **3e** (Table 1). **5e** showed a reversible crystal–crystal transition that was observed at 60 °C on first heating, and at 52 °C on the second heating cycle (shown in Figure 2) followed by melting at 79 °C. Only a single crystallization peak, at 20 °C, was observed in the cooling scan.

The tetrazolate salt, **3g**, also displayed a reversible solid-solid transition at 83 °C. A solid–solid transition at 49 °C was observed in the first heating scan only for **4g**.

The most striking evidence for polymorphism was found in the 4-nitro-1,2,3-triazolate salt **4b**, which was obtained as a low-temperature monotropic polymorph from solution. On heating, the salt appears to melt at 30 °C to form a clear viscous phase, which transforms on standing to a more stable solid polymorph. This transition is observed in the DSC trace as a first-order endothermic peak on the first heating cycle. After cooling and on the second heating, a more stable polymorph (reversible m.p. 82 °C, crystallizing at 63 °C) is obtained (Figure 3).

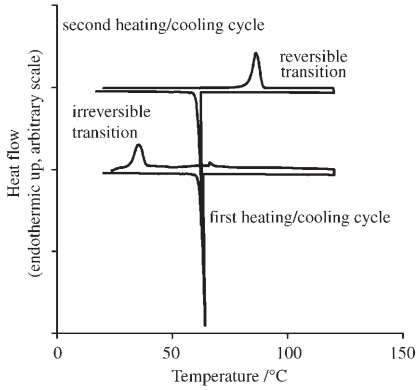

Figure 3. Characteristic DSC traces for the tetraethylammonium 4-nitro-1,2,3-triazolate (**4b**) showing the polymorphic behavior of the characterized salt. Transitions are shown from the first and second heating and cooling cycles to indicate the differences in the melting points of the polymorphs.

Thermal stability was measured by using thermogravimetric analysis (TGA), with isocratic heating at 5 °C min^{-1} under an inert argon atmosphere. All the salts prepared were thermally stable to greater than 200 °C, except for the 4-nitro-1,2,3-triazolates (**3–6**)**b**, which started to decompose between 180 and 219 °C (Table 1). The decomposition temperatures shown in Table 1 were determined from both the onset to 5 wt % mass loss in an isocratic TGA experiment, and from the inflection point for complete decomposition, and all showed a single-step decomposition profile. The salts show a slight increase in upper stability temperature on increasing the cation alkyl chain from methyl to butyl, and on changing from ammonium to imidazolium cations. However, the increased stability is relatively small and is probably not significant. The high-melting tetramethylammonium salts all showed the onset of decomposition around the melting points, whereas appreciable liquid ranges could be obtained with the larger cations, most notably with $[C_4mim]^+$, with liquidus ranges from sub-ambient to above 150 °C.

The melting points (and T_g points for noncrystallizing salts) varied most significantly with change in the size and shape of the organic cation, as anticipated, in that they decreased with increasing cation size and with much less varia-

tion than was found with anion type. The liquid ranges for each salt, determined from the lower melting transition through to the decomposition temperatures, are shown in Figure 4 grouped by anion type. It can be clearly seen that

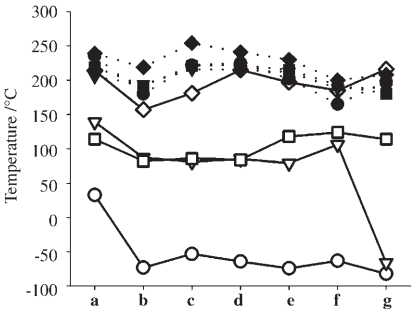

Figure 4. Liquid range from melting or glass-transition points (open symbols) to onset of decomposition (filled symbols) for (**3**–**6**)**a**–**g**, showing the significant changes in thermal range and stability with variation in cation ($[NMe_4]^+$ (**3**), diamond; $[NEt_3]^+$ (**4**), square; $[NBu_4]^+$ (**5**), triangle; $[C_4mim]^+$ (**6**), circle) and the relatively small variation with anion.

for each cation (**3**–**6**), the melting and decomposition temperatures measured are largely invariant with anion. Two observations are worth noting, first that all the anions studied could be used to form low-melting ILs, and that with each cation type, the 4-nitro-1,2,3-triazolate anion (**b**) yielded salts with the lowest melting points.

Comparison of the thermal properties of azolate ILs (**3**–**6**)**a**–**g** with data for the corresponding bistriflimides, triflates, and tetrafluoroborate salts (Table 1) shows that introduction of the flat heterocyclic azolate anion tends to lead to salts with melting points that are either comparable to or lower than those for the bistriflimide salts. The most significant depression of melting points was observed for the azolates versus triflates and tetrafluoroborates in the tetraethyl- and tetramethylammonium salts.

It can be clearly seen that the liquid range for these ILs is governed principally by the choice of cation, which has the greatest influence on the lower melting (or glass) transition temperature, with the $[C_4mim]^+$ salts **6a**–**g** showing the lowest temperatures of all.

X-ray crystallography: Crystals suitable for X-ray structure analysis were obtained for six of the anions with tetraalkylammonium cations (**4a**, **3c**, **5c**, **5d**, **4e**, and **4f**) by trituration and slow crystallization from dichloromethane/diethyl ether (Table 2). All non-hydrogen atoms were fully refined anisotropically and all hydrogen atoms were refined isotropically, except for the hydrogen atoms in the disordered **3c**. The six structurally characterized salts are depicted in Figures 5 and 6 with an ORTEP view of each asymmetric unit (displayed such that the hydrogen-bonding contact most under the van der Waals separation is noted) and a packing diagram.

Salt **3c** was the only structure to exhibit disorder, and only one of the cations in this structure is disordered. Three of the four methyl groups on the disordered cation are rotationally displaced with occupancies of 70:30. As in **4a**, the cations and anions form discrete ionic columns. In **3c** the two positions for the disordered carbon atoms have different close contacts: 2.38 Å for C72−H72B···O32 and 2.50 Å for C72A−H72E···O12 (Table 3).

Structures **3c** and **5c** were the only structures to crystallize with more than one cation and anion per unit cell. As mentioned above, one difference in the two cations in **3c** is the disorder, however, there is also a difference in the close contacts between the ions. The nondisordered cation in **3c**

Table 2. Crystallographic data.

	4a	**3c**	**5c**	**5d**	**4e**	**4f**
color/shape	colorless/platelet	yellow/platelet	colorless/fragment	yellow/fragment	colorless/fragment	colorless/fragment
formula	$C_{10}H_{20}N_6O_4$	$C_7H_{13}N_5O_4$	$C_{19}H_{37}N_5O_4$	$C_{19}H_{37}N_5O_4$	$C_{13}H_{21}N_5$	$C_{11}H_{22}N_4O_2$
M_r	288.3	231.22	399.54	399.54	247.35	242.33
crystal system	orthorhombic	orthorhombic	triclinic	monoclinic	orthorhombic	monoclinic
space group	$P2_12_12_1$ (no. 19)	*Pnma* (no. 62)	$P\bar{1}$ (no. 2)	$P2_1/c$ (no. 14)	*Pbcm* (no. 57)	$P2_1/n$ (no. 12)
T [K]	173	173	173	173	173	173
a [Å]	6.9962(17)	9.810(5)	12.278(4)	12.428(3)	7.902(2)	14.391(4)
b [Å]	12.148(3)	19.469(9)	13.596(5)	11.967(3)	15.154(5)	12.516(3)
c [Å]	16.572(4)	16.745(8)	13.628(5)	15.047(4)	12.082(4)	7.5669(17)
α [°]	90	90	90.477(6)	90	90	90
β [°]	90	90	95.765(7)	91.644(4)	90	106.380(3)
γ [°]	90	90	91.929(7)	90	90	90
V [Å^3]	1408.5(6)	3198(3)	2262.0(14)	2237.0(10)	1446.8(8)	1307.6(6)
Z	4	12	4	4	4	4
ρ_{calcd} [g cm^{-3}]	1.360	1.441	1.173	1.186	1.136	1.231
independent/ obsd reflns	2021 (R_{int} = 0.0145)/ 1957 ($[I>2\sigma]$)	2377 (R_{int} = 0.0285)/ 1962 ($[I>2\sigma]$)	6508 (R_{int} = 0.0188)/ 4726 ($[I>2\sigma]$)	3216 (R_{int} = 0.0138)/ 2871 ($[I>2\sigma]$)	1095 (R_{int} = 0.0276)/ 1016 ($[I>2\sigma]$)	1763 (R_{int} = 0.0393)/ 865 ($[I>2\sigma]$)
GooF	1.073	1.072	1.062	1.033	1.030	1.018
R_1, wR_2[a] $[I>2\sigma(I)]$	0.0198, 0.0486	0.0804, 0.2202	0.0525, 0.1445	0.0312, 0.0774	0.0285, 0.0705	0.0509, 0.1575
R_1, wR_2[a] (all data)	0.0207, 0.0493	0.0909, 0.2325	0.0710, 0.1626	0.0360, 0.0807	0.0311, 0.0725	0.0806, 0.1855

[a] $R = \Sigma||F_o|-|F_c||/\Sigma|F_o|$. $R_2 = \{\Sigma[w(F_o^2-F_c^2)^2]/\Sigma(w(F_o^2)^2]\}^{1/2}$.

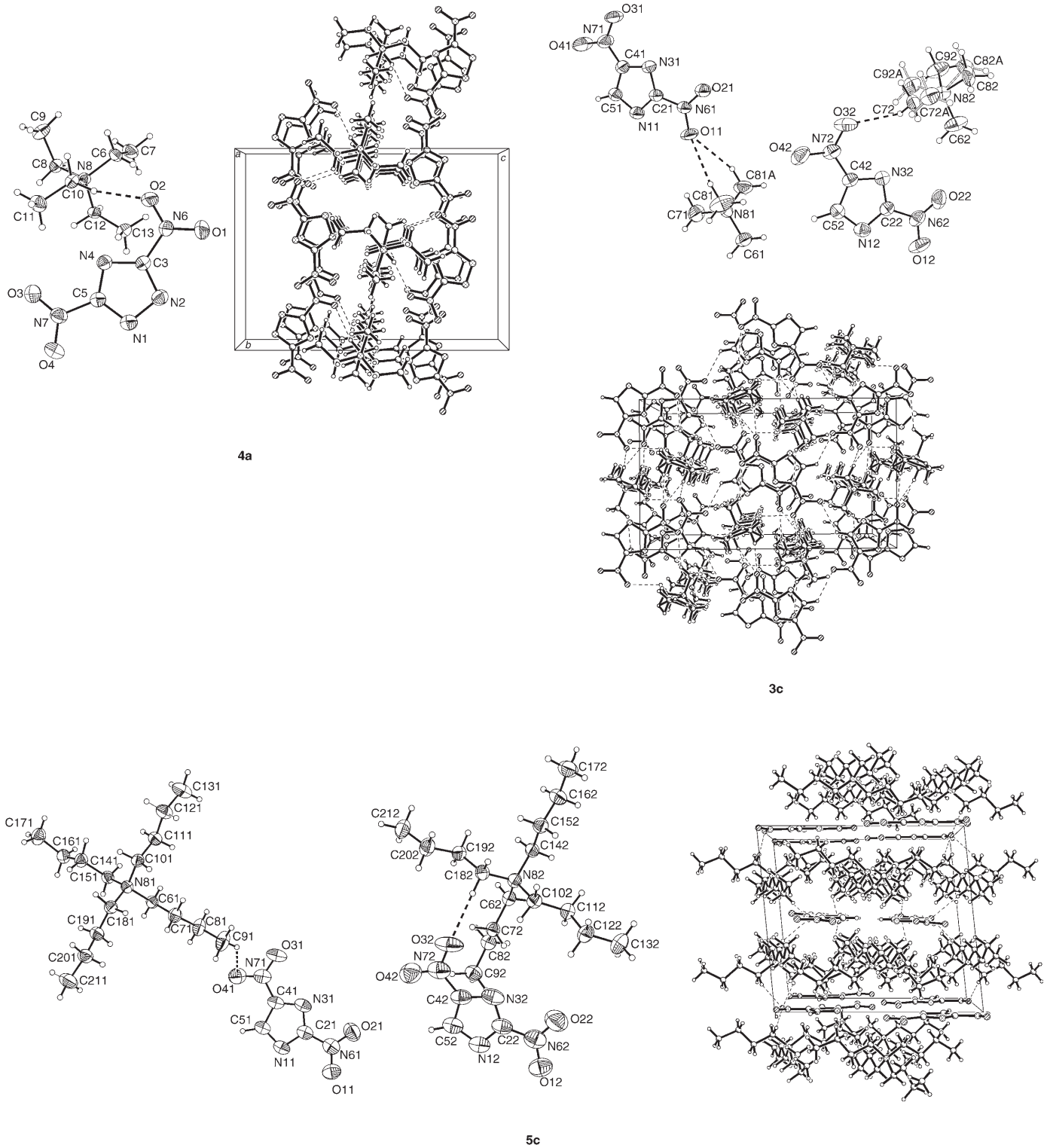

Figure 5. ORTEP views of the asymmetric units and packing diagrams for tetraethylammonium 3,5-dinitro-1,2,4-triazolate (**4a**), tetramethylammonium 2,4-dinitroimidazolate (**3c**), and tetrabutylammonium 2,4-dinitroimidazolate (**5c**).

has a longer cation–anion shortest contact at 2.62 Å, versus the 2.38 and 2.50 Å close contacts for the disordered cation.

On close examination of the cations and anions in **5c**, there is little difference in conformation of the individual cations and anions, but as shown in Figure 5, there is a difference in the close contacts between the cation and anion of the two unique IL formula units. The two closest anion/cation contacts are C91–H91A···O41 (2.62 Å) and C182–H18C···O32 (2.35 Å). This difference in close contacts disrupts any higher-order symmetry that would be possible in

Table 3. Cation···anion close-contact geometries.[a]

	Hydrogen type	D−H···A	D−H [Å]	H···A [Å]	−ΔvdW	D···A [Å]	D−H···A [°]	Symmetry code
4a	N−*CH*$_2$CH$_3$	C10−H10B···O2	1.010(16)	2.408(16)	−0.31	3.3952(17)	165.5(11)	
		C12−H12A···O1	0.948(13)	2.552(12)	−0.17	3.2001(18)	125.8(9)	1−*x*, −0.5+*y*, 1.5−*z*
3c[b]	N−*CH*$_3$	C72−H72B···O32	0.98	2.38	−0.34	2.828(11)	106.9	
		C92−H92B···O32	0.98	2.41	−0.31	3.072(11)	124.4	−*x*, 1−*y*, 1−*z*
		C82−H82A···O41	0.98	2.49	−0.23	2.983(12)	110.8	−0.5−*x*, 1−*y*, −0.5+*z*
		C72A−H72E···O12	0.98	2.50	−0.22	3.386(6)	150.7	−1+*x*, *y*, *z*
		C62−H62C···O22	0.98	2.53	−0.19	3.299(5)	134.9	
		C92−H92B···O12	0.98	2.56	−0.16	3.440(13)	148.9	−1+*x*, *y*, *z*
		C82−H82B···O31	0.98	2.58	−0.14	3.177(11)	119.4	−1−*x*, 1−*y*, 1−*z*
		C81−H81C···O11	0.98	2.62	−0.11	3.520(5)	152.8	
		C82A−H82E···O12	0.98	2.62	−0.11	3.486(6)	146.8	−1+*x*, *y*, *z*
5c	N−*CH*$_2$-	C182−H18C···O32	0.98(2)	2.35(2)	−0.37	3.325(3)	174.0(16)	
		C142−H14C···O31	0.98(2)	2.43(2)	−0.29	3.403(3)	173.3(16)	*x*, *y*, 1+*z*
		C182−H18D···O32	0.97(2)	2.45(2)	−0.27	3.400(3)	166.8(16)	1−*x*, 1−*y*, 2−*z*
		C62−H62B···O31	0.98(2)	2.52(2)	−0.19	3.459(3)	158.9(15)	*x*, 1−*y*, 1−*z*
		C142−H14D···O31	0.98(2)	2.55(2)	−0.18	3.458(3)	155.6(15)	
		C101−H10A···N12	1.02(2)	2.65(2)	−0.10	3.669(3)	172.5(15)	1−*x*, 1−*y*, 1−*z*
	-*CH*$_3$	C131−H13A···O42	1.01(3)	2.58(3)	−0.12	3.411(4)	140(2)	
		C171−H17C···O41	1.00(3)	2.62(3)	−0.10	3.457(3)	141.0(19)	−*x*, −*y*, 1−*z*
5d	N−*CH*$_2$-	C18−H18A···O1	0.961(14)	2.440(15)	−0.28	3.3311(19)	154.2(11)	
		C14−H14B···O3	0.986(13)	2.462(14)	−0.26	3.4202(19)	164.0(10)	*x*, 0.5−*y*, 0.5+*z*
		C6−H6A···O2	0.968(14)	2.466(14)	−0.26	3.3362(18)	149.5(10)	−*x*, −0.5+*y*, 1.5−*z*
		C10−H10A···N3	0.972(14)	2.498(14)	−0.25	3.4550(19)	168.4(10)	
4e	N−*CH*$_2$CH$_3$	C10−H10B···N3	0.977(12)	2.613(12)	−0.14	3.5043(17)	151.6(8)	
		C8−H8A···N7	0.961(12)	2.641(13)	−0.12	3.5089(18)	150.4(8)	2−*x*, −0.5+*y*, 0.5−*z*
		C10−H10A···N1	0.987(12)	2.650(13)	−0.11	3.6013(18)	162.0(8)	1−*x*, −0.5+*y*, 0.5−*z*
4f	N−*CH*$_2$CH$_3$	C12−H12B···N3	0.99(3)	2.50(3)	−0.24	3.443(5)	158(3)	
		C8−H8B···N3	0.90(3)	2.58(3)	−0.18	3.459(6)	164(3)	−2−*x*, 2−*y*, 1−*z*
	N−CH$_2$*CH*$_3$	C11−H11B···O2	1.05(3)	2.54(3)	−0.20	3.441(6)	144(2)	−2.5−*x*, −0.5+*y*, 1.5−*z*
		C11−H11A···O1	1.03(4)	2.61(4)	−0.11	3.354(6)	129(3)	
		C9−H9C···O2	1.08(5)	2.64(5)	−0.11	3.711(7)	169(4)	−3−*x*, 2−*y*, 1−*z*

[a] The contacts included in this table are those at least 0.1 Å under the van der Waals (vdW) separation. [b] The hydrogen atoms of **3c** were constrained due to the presence of disorder.

these highly symmetric ions, resulting in a low-symmetry (triclinic) space group.

Bond lengths and angles of the azolate anions are shown in Table 4. A comparison of the imidazolate anions (**3c**, **4e**, **4f**, **5c**, and **5d**) indicates that there is little effect of substitution on the bond lengths and angles in the ring.

The nitro substituents in the structures of **4a**, **3c**, **5c**, **5d**, and **4f** exhibit some twisting out of the plane of the ring (Table 5) ranging from a slight twist in **4a**, **3c**, **5c**, and **4f** to 32.73 and 17.95° in **5d**. The observation of larger twist angles for the nitro groups in **5d** is consistent with the steric hindrance inherent in the 4,5-substituted ring.

Table 4. Bond lengths [Å] and angles [°] in the azolate rings.

	4a		**3c**		**5c**		**5d**	**4e**	**4f**
N(1)−N(2)	1.3585(16)	N(1)−C(2)	1.343(5)	1.340(4)	1.354(3)	1.359(3)	1.348(2)	1.342(2)	1.371(4)
N(2)−C(3)	1.3326(16)	C(2)−N(3)	1.325(5)	1.324(4)	1.324(3)	1.329(3)	1.3370(19)	1.340(2)	1.326(4)
C(3)−N(4)	1.3329(17)	N(3)−C(4)	1.349(6)	1.344(4)	1.335(3)	1.336(3)	1.3438(17)	1.3595(19)	1.360(3)
N(4)−C(5)	1.3258(16)	C(4)−C(5)	1.381(6)	1.386(5)	1.386(3)	1.392(3)	1.3907(19)	1.389(2)	1.388(4)
C(5)−N(1)	1.3323(17)	C(5)−N(1)	1.346(6)	1.346(5)	1.337(3)	1.345(3)	1.3409(18)	1.358(2)	1.343(4)
N(1)-N(2)-C(3)	103.93(10)	N(1)-C(2)-N(3)	118.8(4)	119.2(3)	118.8(2)	118.5(2)	116.91(13)	116.59(14)	116.5(3)
N(2)-C(3)-N(4)	117.10(11)	C(2)-N(3)-C(4)	99.4(4)	99.5(3)	99.59(19)	99.9(2)	102.15(11)	102.64(13)	101.4(2)
C(3)-N(4)-C(5)	97.64(10)	N(3)-C(4)-C(5)	112.3(4)	111.9(3)	112.3(2)	112.4(2)	109.43(11)	109.00(13)	111.2(2)
N(4)-C(5)-N(1)	117.35(11)	C(4)-C(5)-N(1)	107.5(4)	107.8(3)	107.9(2)	107.7(2)	109.63(12)	109.35(13)	107.9(2)
C(5)-N(1)-N(2)	103.98(10)	C(5)-N(1)-C(2)	102.0(4)	101.6(3)	101.40(19)	101.5(2)	101.87(12)	102.42(13)	103.0(2)

Table 5. Torsion angles [°] for the NO_2 groups in the anions.

	4a		3c	5c		5d	4f
N(2)-C(3)-N(6)-O(1)	−5.97(17)	N(11)-C(21)-N(61)-O(11)	0.000(1)	179.9(2)	N(1)-C(5)-N(7)-O(4)	−32.73(18)	–
			−0.1(4)	−5.3(3)			
N(2)-C(3)-N(6)-O(2)	173.53(11)	N(11)-C(21)-N(61)-O(21)	180.0	0.4(3)	N(1)-C(5)-N(7)-O(3)	145.36(13)	–
			179.5(3)	175.6(2)			
N(1)-C(5)-N(7)-O(3)	−178.67(12)	N(31)-C(41)-N(71)-O(31)	0.000(1)	−4.7(3)	N(3)-C(4)-N(6)-O(1)	−17.95(19)	1.4(6)
			−1.9(4)	1.1(3)			
N(1)-C(5)-N(7)-O(4)	2.72(17)	N(31)-C(41)-N(71)-O(41)	180.000(1)	174.77(19)	N(3)-C(4)-N(6)-O(2)	162.87(12)	−178.9(4)
			178.2(3)	−178.6(2)			

Three related crystal structures of simple nitroazolate anions were found in the Cambridge Crystallographic Database:[23] a sodium 2-nitroimidazolate complex with [15]crown-5,[24] potassium 4,5-dinitroimidazolate,[25] and 1,8-bis(dimethylamino)naphthalene 2,4-dinitroimidazolate.[26] In the 1,8-bis(dimethylamino)naphthalene salt of 2,4-dinitroimidazolate (anion **c**), the C(2)−NO_2 group of the anion resides in the plane of the ring, however, the C(4)−NO_2 group is twisted out of the anion plane (dihedral angle = 13.61°), whereas the maximum deviation of either nitro group from the plane of the anion in **5c** is 5.62°. The anion ring in potassium 4,5-dinitroimidazolate has both nitro groups twisted out of the heterocycle ring plane, with dihedral angles of 14.0 and 14.31° (compared with 14.13 and 32.19° in **5d**).

What is most obvious from the packing diagrams of **5c**, **4e**, and **4f** (Figures 5 and 6) is that the salts crystallize in layered structures, forming sheets of anions separated by layers of tetraethylammonium or tetrabutylammonium cations that close-pack at the van der Waals separation distances. The cations flatten out into an oblate conformation that enables maximum space filling within the layers, and a number of short hydrogen-bonding contacts from the most polar hydrogen-bond donor positions on the cations, adjacent to the hetero atom, to the most basic sites of the anions.

In contrast to the layered structures described above, **5d** forms a close-packed crystalline phase with each ion surrounded by five counterions. The out of plane nitro groups are good hydrogen-bond acceptors and contribute to relatively short hydrogen bonds with α-hydrogen atoms on the cations. The tetrabutylammonium cations have extended alkyl chains, closer to tetrahedral symmetry (terminal CH_3–CH_3 distances are 8.25 ± 1.03 Å) relative to the other structures here.

The smaller tetramethylammonium cation in **3c** prevents efficient formation of an insulating cation layer between sheets of anions (in contrast to **5c**). Instead, a layered structure with both cations and anions in each layer is observed.

In **4a**, the nitrogen and carbon atoms of the triazolate anion ring are planar, with both nitro groups also in the plane of the ring. The cations and anions form an ordered alternating array held together primarily by Coulombic interactions. The three shortest and most significant cation–anion close contacts are C4−H···N3 (2.60 Å), C5−H···O2 (2.41 Å), and C7−H···O1 (2.54 Å).

A unique aspect of the anions in these structures is their potential to form anion–anion hydrogen-bonding interactions, and the salts **3c**, **4e**, and **4f** exhibit such close contacts (Table 6). In **3c** the interactions are between the C5 hydrogen atoms on both anions to a nitro group oxygen of an adjacent anion (Figure 5). The anions in the tetraethylammonium salts **4e** and **4f** interact in a head to tail fashion forming planes with C2−H···N (cyano) or C2−H···O (nitro) close contacts, respectively (Figure 6).

The anions in **4a**, **5c**, and **5d** have no similar close anion–anion interactions. The anion in **4a** lacks a hydrogen-bond donor. In the structures **5c** and **5d**, the larger tetrabutylammonium cations appear to more effectively separate the anions in the lattice.

Conclusion

Challenges facing the preparation of energetic ILs based on ring-substituted heterocyclic cations result from the destabilization of the aromatic core by substitution with electron-withdrawing groups (such as nitro or nitrile). In contrast, the electron-withdrawing characteristics of these same functional groups can be utilized to prepare correspondingly stabilized anionic azolate anions, which leads to opportunities to form ILs containing heterocyclic anions. A wide range of heterocyclic anions can be used to prepare ILs and fifteen such examples have been illustrated here: seven from all combinations of $[C_4mim]^+$ and the seven heterocyclic azolate anions studied, six from combinations of tetraethyl- or tetrabutylammonium cations and anions **b**, **c**, and **d**, and two additional ionic liquids from the combination of tetrabutylammonium with **e** and **g**.

It is most interesting that ILs can be readily formed with *N*-heterocyclic cations and anions. The $[C_4mim]^+$ azolates are liquid at room temperature (except for the low melting 3,5-nitrotriazolate), with tetraalkylammonium azolates showing melting points lower than those of the corresponding triflates and tetrafluoroborates, especially in the tetramethyl- and tetraethylammonium series, and comparable with corresponding bistriflimides. Efficient packing, and subsequent crystallization, presumably is suppressed by the introduction of *N*-alkyl substituents, which block close π–π stacking of cations and anions. In the structures of the tet-

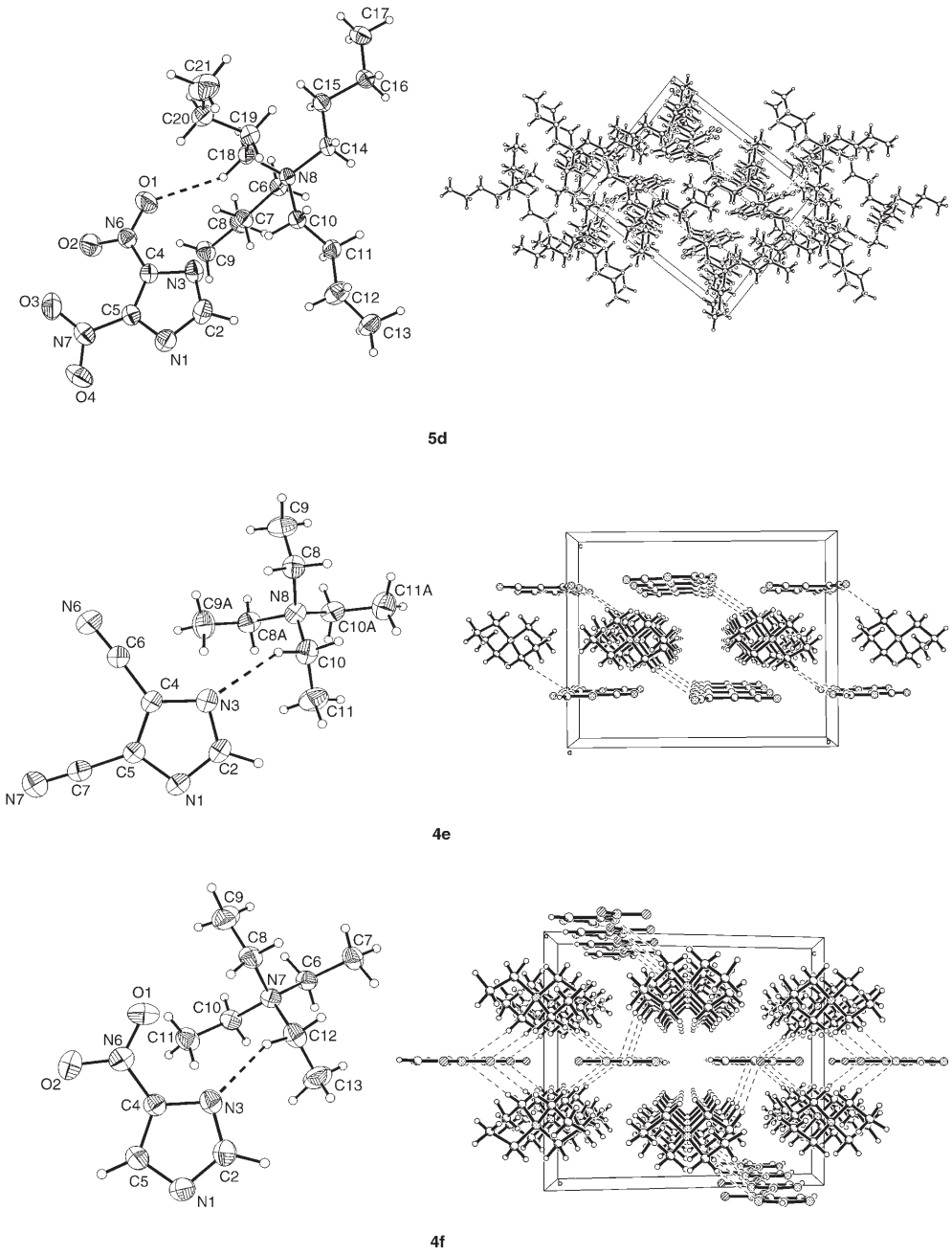

Figure 6. ORTEP views of the asymmetric units and packing diagrams for tetrabutylammonium 4,5-dinitroimidazolate (**5d**), tetraethylammonium 4,5-dicyanoimidazolate (**4e**), and tetraethylammonium 4-nitroimidazolate (**4f**).

Table 6. Anion···anion close-contact geometries.[a,b]

	Hydrogen type	D−H···A	D−H [Å]	H···A [Å]	−ΔvdW	D···A [Å]	D−H···A [°]
3c	C−*H*	C51−H51A···O41	0.97(4)	2.55(4)	−0.17	3.227(6)	127(3)
		C52−H52B···O42	0.99(4)	2.54(3)	−0.17	3.236(5)	127(2)
4e	C−*H*	C2−H2A···N6	0.996(16)	2.420(17)	−0.33	3.406(2)	170.6(12)
4f	C−*H*	C2−H2A···O2	1.01(3)	2.36(3)	−0.36	3.356(5)	172(2)

[a] The contacts included in this table are those at least 0.1 Å under the van der Waals (vdW) separation. [b] Compounds **4a**, **5c**, and **5d** have no anion–anion close contacts.

raalkylammonium salts, flattening of the cations into an oblate form allows enhanced ion–ion packing.

Experimental Section

Caution! Although no problems were encountered during this work, the introduction of energetic functionalities into heterocyclic compounds has inherent risks and appropriate procedures must be taken and all materials must be handled with extreme care.

General methods: Melting points were determined on a hot-stage apparatus and are uncorrected. NMR spectra were recorded in $CDCl_3$ (unless otherwise stated) at 25 °C with tetramethylsilane (TMS) as the internal

standard for ^{1}H (300 MHz) or the solvent as the internal standard for ^{13}C (75 MHz). All of the chemicals were employed as supplied.

Materials: Potassium 3,5-dinitro-1,2,4-triazolate (**2a**) was prepared (in 46% yield) according to the published one-pot procedure by the reaction of cyanoguanidine with hydrazine followed by diazotization of intermediate 3,5-diamino-1,2,4-triazole and substitution at the diazonium group.[27] 4-Nitro-1,2,3-triazole (**1b**) was prepared according to a published procedure from 2-phenyl-1,2,3-triazole by trinitration followed by treatment of intermediate 2-(2,4-dinitrophenyl)-4-nitro-1,2,3-triazole with sodium methoxide in methanol under reflux.[28] 2,4-Dinitroimidazole (**1c**) was prepared by N-nitration[29,30] of 4-nitroimidazole (**1f**) followed by isomerization of the intermediate 1,4-dinitroimidazole in chlorobenzene at 115°C.[31] 4,5-Dinitroimidazole (**1d**) was prepared by nitration of 4-nitroimidazole with fuming nitric acid in concentrated sulfuric acid under reflux.

Procedure for the preparation of 4,5-dinitroimidazole (1d): A mixture of concentrated sulfuric acid (10 mL) and fuming nitric acid (90%, 8 mL, 0.17 mol) was added to 4-nitroimidazole (**1f**) (2.0 g, 18 mmol) dissolved in a minimum quantity of concentrated sulfuric acid. The mixture was heated under reflux for 5 h. After cooling, the mixture was poured into ice, and the pH was adjusted to 2 by the addition of sodium bicarbonate. The product was extracted with ethyl acetate. The extract was concentrated to give 4,5-dinitroimidazole (**1d**) as yellow crystals from water (1.55 g, 55%). M.p. 166–169°C (ref. [30]: 188–189°C); ^{1}H NMR ([D$_6$]DMSO): δ = 12.37 (brs, 1H), 8.06 ppm (s, 1H); ^{13}C NMR ([D$_6$]DMSO): δ = 135.5, 134.9 ppm.

General procedure for the preparation of potassium azolates 2a–d: Potassium carbonate (0.85 g, 6 mmol) was added to a solution of the appropriate azole (4 mmol) in acetone (40 mL) (Figure 1 and Scheme 1). The mixture was stirred at 20°C for 6 h, filtered, and the precipitate was washed with acetone. The solvent was evaporated and the residue was dried under vacuum to give potassium azolates **2a–d**.

General procedure for the preparation of azolates (3–6)a–d: A solution of the appropriate tetraalkylammonium or imidazolium halide (3 mmol) in dichloromethane (30 mL) was added to a solution of the potassium azolate **2a–d** (3 mmol) in acetone (30 mL) at 20–25°C. The reaction mixture was stirred for 3 h (24 h for the preparation of tetramethylammonium salts **3a–d**). The resultant precipitate of potassium halide was removed by using filtration and the solvent was evaporated under vacuum. The residue was dried under vacuum. The product was extracted with acetone, the extract was filtered, and the solvent was removed to give (**3–6**)**a–d**.

General procedure for the preparation of azolates (3–6)e–g: Anhydrous potassium carbonate (0.7 g, 5 mmol) was added to a solution of the appropriate azole **1e–g** (3 mmol) in acetone (30 mL) and the mixture was stirred for 10 min at 20–25°C. Then a solution of the appropriate tetraalkylammonium or imidazolium halide (3 mmol) in dichloromethane (30 mL) was added and the reaction mixture was stirred for 3 h (24 h for the preparation of tetramethylammonium salts **3e–g**). The mixture was filtered and concentrated under vacuum. The product was extracted with acetone, the extract was filtered, and the solvent was removed to give (**3–6**)**e–g**.

Tetramethylammonium 3,5-dinitro-1,2,4-triazolate (3a): Microcrystals from acetone (84%); m.p. 219–221°C; ^{1}H NMR: δ = 3.13 ppm (s, 12H); ^{13}C NMR: δ = 54.4 (t, J = 4.0 Hz, 4C), 162.9 ppm (2C); elemental analysis calcd (%) for $C_6H_{12}N_6O_4$ (232.2): C 31.04, H 5.21, N 36.19; found: C 31.41, H 5.17, N 36.20.

Tetramethylammonium 4-nitro-1,2,3-triazolate (3b): Microcrystals from acetone (92%); m.p. 124–126°C; ^{1}H NMR ([D$_6$]DMSO): δ = 3.13 (s, 12H), 8.05 ppm (s, 1H); ^{13}C NMR ([D$_6$]DMSO): δ = 54.4 (t, J = 4.0 Hz, 4C), 129.5, 154.1 ppm; elemental analysis calcd (%) for $C_6H_{13}N_5O_2$ (187.2): C 38.50, H 7.00, N 37.41; found: C 38.81, H 7.08, N 37.36.

Tetramethylammonium 2,4-dinitroimidazolate (3c): Microcrystals (83%); m.p. 178–180°C; ^{1}H NMR ([D$_6$]DMSO): δ = 3.13 (s, 12H), 7.75 ppm (s, 1H); ^{13}C NMR ([D$_6$]DMSO): δ = 54.4 (t, J = 4.0 Hz, 4C), 130.1, 146.8, 154.1 ppm; elemental analysis calcd (%) for $C_7H_{13}N_5O_4$ (231.2): C 36.36, H 5.67, N 30.29; found: C 36.69, H 5.76, N 29.79.

Tetramethylammonium 4,5-dinitroimidazolate (3d): Microcrystals from acetone (98%); m.p. 215–218°C; ^{1}H NMR ([D$_6$]DMSO): δ = 3.11 (s, 12H), 6.99 ppm (s, 1H); ^{13}C NMR ([D$_6$]DMSO): δ = 54.4 (t, J = 4.0 Hz, 4C), 139.4, 140.3 ppm (2C); elemental analysis calcd (%) for $C_7H_{13}N_5O_4$ (231.2): C 36.36, H 5.67, N 30.29; found: C 36.51, H 5.71, N 30.46.

Tetramethylammonium 4,5-dicyanoimidazolate (3e): Microcrystals from acetone (98%); m.p. 197–199°C; ^{1}H NMR ([D$_6$]DMSO): δ = 3.11 (s, 12H), 7.31 ppm (s, 1H); ^{13}C NMR ([D$_6$]DMSO): δ = 54.4 (t, J = 4.0 Hz, 4C), 116.9, 117.5, 148.8 ppm; elemental analysis calcd (%) for $C_9H_{13}N_5$ (191.2): C 56.53, H 6.85, N 36.62; found: C 54.95, H 7.18, N 35.79.

Tetramethylammonium 4-nitroimidazolate (3f): White microcrystals (91%); m.p 170–172°C; ^{1}H NMR ([D$_6$]DMSO): δ = 3.11 (s, 12H), 7.09 (s, 1H), 7.71 ppm (s, 1H); ^{13}C NMR ([D$_6$]DMSO): δ = 54.4 (t, J = 4.0 Hz, 4C), 131.6, 137.4, 146.0 ppm; elemental analysis calcd (%) for $C_7H_{16}N_4O_3$ (186.2): C 41.17, H 7.90, N 27.43; found: C 41.54, H 7.21, N 28.41.

Tetramethylammonium tetrazolate (3g): Microcrystals from acetone (15%); m.p. 216–218°C; ^{1}H NMR ([D$_6$]DMSO): δ = 3.10 (s, 12H), 8.03 ppm (s, 1H); ^{13}C NMR ([D$_6$]DMSO): δ = 54.4 (t, J = 4.0 Hz, 4C), 148.6 ppm; elemental analysis calcd (%) for $C_5H_{13}N_5$ (143.2): C 41.94, H 9.15, N 48.91; found: C 42.36, H 9.53, N 47.67.

Tetraethylammonium 3,5-dinitro-1,2,4-triazolate (4a): Colorless crystals from dichloromethane/diethyl ether (94%); m.p. 104–106°C; ^{1}H NMR: δ = 1.40 (tt, J = 7.3, 1.6 Hz, 12H), 3.46 ppm (q, J = 7.3 Hz, 8H); ^{13}C NMR: δ = 7.5 (4C), 52.6 (t, J = 2.9 Hz, 4C), 163.3 ppm (2C); elemental analysis calcd (%) for $C_{10}H_{20}N_6O_4$ (288.3): C 41.66, H 6.99, N 29.15; found: C 41.79, H 7.12, N 27.34.

Tetraethylammonium 4-nitro-1,2,3-triazolate (4b): Microcrystals from acetone (99%); m.p. 30–31°C; ^{1}H NMR: δ = 1.30 (tt, J = 7.3, 1.7 Hz, 12H), 3.31 (q, J = 7.3 Hz, 8H), 8.16 ppm (s, 1H); ^{13}C NMR: δ = 7.3 (4C), 52.3 (t, J = 2.9 Hz, 4C), 130.0, 154.5 ppm; elemental analysis calcd (%) for $C_{10}H_{21}N_5O_2$ (243.3): C 49.36, H 8.70, N 28.78; found: C 48.26, H 8.84, N 27.95.

Tetraethylammonium 2,4-dinitroimidazolate (4c): Microcrystals (97%); m.p. 76–78°C; ^{1}H NMR: δ = 1.36 (tt, J = 7.3, 1.5 Hz, 12H), 3.40 (q, J = 7.3 Hz, 8H), 7.79 ppm (s, 1H); ^{13}C NMR: δ = 7.3 (4C), 52.5 (t, J = 2.9 Hz, 4C), 130.7, 147.3, 154.3 ppm; elemental analysis calcd (%) for $C_{11}H_{21}N_5O_4$ (287.3): C 45.98, H 7.37, N 24.37; found: C 45.54, H 7.57, N 23.85.

Tetraethylammonium 4,5-dinitroimidazolate (4d): Microcrystals from acetone (96%); m.p. 101–103°C; ^{1}H NMR: δ = 1.32 (tt, J = 7.3, 1.6 Hz, 12H), 3.28 (q, J = 7.3 Hz, 8H), 7.09 ppm (s, 1H); ^{13}C NMR: δ = 7.3 (4C), 52.5 (t, J = 2.9 Hz, 4C), 139.9, 140.1, 140.6 ppm; elemental analysis calcd (%) for $C_{11}H_{21}N_5O_4$ (287.3): C 45.98, H 7.37, N 24.37; found: C 45.78, H 7.57, N 23.60.

Tetraethylammonium 4,5-dicyanoimidazolate (4e): Microcrystals from acetone (85%); m.p. 129–131°C; ^{1}H NMR: δ = 1.33 (tt, J = 7.3, 1.8 Hz, 12H), 3.25 (q, J = 7.3 Hz, 8H), 7.46 ppm (s, 1H); ^{13}C NMR: δ = 7.4 (4C), 52.5 (t, J = 2.9 Hz, 4C), 117.1, 118.4, 149.2 ppm; elemental analysis calcd (%) for $C_{13}H_{21}N_5$ (247.3): C 63.13, H 8.56, N 28.31; found: C 63.04, H 8.79, N 28.32.

Tetraethylammonium 4-nitroimidazolate (4f): Microcrystals (78%); m.p. 124–126°C; ^{1}H NMR: δ = 1.24 (tt, J = 7.3, 1.6 Hz, 12H), 3.18 (q, J = 7.3 Hz, 8H), 7.33 (s, 1H), 7.93 ppm (s, 1H); ^{13}C NMR: δ = 7.2 (4C), 52.3 (t, J = 2.9 Hz, 4C), 132.2, 146.7, 148.3 ppm; elemental analysis calcd (%) for $C_{11}H_{22}N_4O_2$ (242.3): C 54.52, H 9.15, N 23.12; found: C 53.43, H 9.27, N 22.68.

Tetraethylammonium tetrazolate (4g): Microcrystals from acetone (81%); m.p. 94–96°C; ^{1}H NMR: δ = 1.21 (tt, J = 7.3, 1.8 Hz, 12H), 3.12 (q, J = 7.3 Hz, 8H), 8.35 ppm (s, 1H); ^{13}C NMR: δ = 7.3 (4C), 52.1 (t, J = 2.9 Hz, 4C), 149.8 ppm; elemental analysis calcd (%) for $C_9H_{21}N_5$ (199.3): C 54.24, H 10.62, N 35.14; found: C 53.55, H 11.18, N 33.60.

Tetrabutylammonium 3,5-dinitro-1,2,4-triazolate (5a): Microcrystals from acetone (95%); m.p. 136–138°C; ^{1}H NMR: δ = 0.96 (t, J = 7.3 Hz, 12H), 1.39 (sext, J = 7.3 Hz, 8H), 1.65–1.75 (m, 8H), 3.30–3.36 ppm (m, 8H); ^{13}C NMR: δ = 13.4 (4C), 19.6 (4C), 23.8 (4C), 58.8 (4C),

163.3 ppm (2C); elemental analysis calcd (%) for $C_{18}H_{36}N_6O_4$ (400.5): C 53.98, H 9.06, N 20.98; found: C 53.36, H 9.07, N 21.51.

Tetrabutylammonium 4-nitro-1,2,3-triazolate (5b): Microcrystals from acetone (82%); m.p. 60–61°C; ^{1}H NMR: δ = 0.97 (t, J = 7.3 Hz, 12H), 1.33–1.45 (m, 8H), 1.55–1.66 (m, 8H), 3.20–3.26 (m, 8H), 8.19 ppm (s, 1H); ^{13}C NMR: δ = 13.4 (4C), 19.5 (4C), 23.7 (4C), 58.6 (4C), 130.0, 154.5 ppm; elemental analysis calcd (%) for $C_{18}H_{39}N_5O_3$ (355.5): C 57.88, H 10.52, N 18.75; found: C 58.63, H 10.28, N 20.96.

Tetrabutylammonium 2,4-dinitroimidazolate (5c): Microcrystals (84%); m.p. 79–81°C; ^{1}H NMR: δ = 0.93–0.98 (m, 12H), 1.37 (sext, J = 7.3 Hz, 8H), 1.62–1.72 (m, 8H), 3.26–3.31 (m, 8H), 7.80 ppm (s, 1H); ^{13}C NMR: δ = 13.4 (4C), 19.6 (4C), 23.7 (4C), 58.8 (4C), 130.7, 147.3, 154.3 ppm; elemental analysis calcd (%) for $C_{19}H_{39}N_5O_5$ (399.5): C 54.65, H 9.41, N 16.77; found: C 54.64, H 9.10, N 18.19.

Tetrabutylammonium 4,5-dinitroimidazolate (5d): Microcrystals from acetone (92%); m.p. 64–65°C; ^{1}H NMR: δ = 0.97 (t, J = 7.3 Hz, 12H), 1.38 (sext, J = 7.2 Hz, 8H), 1.56–1.68 (m, 8H), 3.15–3.21 (m, 8H), 7.08 ppm (s, 1H); ^{13}C NMR: δ = 13.4 (4C), 19.5 (4C), 23.7 (4C), 58.6 (4C), 139.9, 140.7, 141.7 ppm; elemental analysis calcd (%) for $C_{19}H_{39}N_5O_5$ (399.5): C 54.65, H 9.41, N 16.77; found: C 54.93, H 9.26, N 18.23.

Tetrabutylammonium 4,5-dicyanoimidazolate (5e): Microcrystals from acetone (93%); m.p. 69–70°C; ^{1}H NMR: δ = 1.00 (t, J = 7.3 Hz, 12H), 1.41 (sext, J = 7.3 Hz, 8H), 1.56–1.67 (m, 8H), 3.13–3.19 (m, 8H), 7.45 ppm (s, 1H); ^{13}C NMR: δ = 13.4 (4C), 19.5 (4C), 23.7 (4C), 58.7 (4C), 117.1, 118.4, 149.1 ppm; elemental analysis calcd (%) for $C_{21}H_{37}N_5$ (359.6): C 70.15, H 10.37, N 19.48; found: C 70.44, H 10.66, N 20.07.

Tetrabutylammonium 4-nitroimidazolate (5f): Microcrystals (95%); m.p. 103–105°C; ^{1}H NMR: δ = 0.97 (t, J = 7.3 Hz, 12H), 1.37 (sext, J = 7.3 Hz, 8H), 1.49–1.60 (m, 8H), 3.08–3.13 (m, 8H), 7.36 (s, 1H), 7.96 ppm (s, 1H); ^{13}C NMR: δ = 13.4 (4C), 19.5 (4C), 23.7 (4C), 58.5 (4C), 131.9, 146.4, 148.4 ppm; elemental analysis calcd (%) for $C_{19}H_{38}N_4O_2$ (354.5): C 64.37, H 10.80, N 15.80; found: C 63.33, H 11.06, N 16.52.

Tetrabutylammonium tetrazolate (5g): Colorless oil (95%); ^{1}H NMR: δ = 0.96 (t, J = 7.2 Hz, 12H), 1.30–1.42 (m, 8H), 1.47–1.57 (m, 8H), 3.06–3.11 (m, 8H), 8.33 ppm (s, 1H); ^{13}C NMR: δ = 13.1 (4C), 19.1 (4C), 23.3 (4C), 58.0 (4C), 149.2 ppm; elemental analysis calcd (%) for $C_{17}H_{37}N_5$ (311.5): C 65.55, H 11.97, N 22.48; found: C 64.66, H 12.92, N 21.67.

1-Butyl-3-methylimidazolium 3,5-dinitro-1,2,4-triazolate (6a): Pale yellow microcrystals (78%); m.p. 35–36°C; ^{1}H NMR: δ = 0.91 (t, J = 7.4 Hz, 3H), 1.35 (sext, J = 7.3 Hz, 2H), 1.90 (quin, J = 7.4 Hz, 2H), 4.13 (s, 3H), 4.36 (t, J = 7.4 Hz, 2H), 7.56 (s, 1H), 7.61 (s, 1H), 9.72 ppm (s, 1H); ^{13}C NMR: δ = 13.1, 19.2, 31.9, 36.4, 49.8, 122.3, 123.8, 136.9, 163.0 ppm (2C); elemental analysis calcd (%) for $C_{10}H_{15}N_7O_4$ (297.3): C 40.80, H 5.09, N 32.98; found: C 40.40, H 5.10, N 32.58.

1-Butyl-3-methylimidazolium 4-nitro-1,2,3-triazolate (6b): Colorless oil (99%); ^{1}H NMR: δ = 0.90 (t, J = 7.3 Hz, 3H), 1.25–1.38 (m, 2H), 1.78–1.88 (m, 2H), 4.04 (s, 3H), 4.26 (t, J = 7.3 Hz, 2H), 7.43 (brs, 1H), 7.47 (brs, 1H), 8.19 (s, 1H), 10.01 ppm (s, 1H); ^{13}C NMR: δ = 13.1, 19.2, 31.8, 36.2, 49.7, 122.0, 123.4, 130.0, 137.4, 154.6 ppm; elemental analysis calcd (%) for $C_{10}H_{16}N_6O_2$ (252.3): C 47.61, H 6.39, N 33.31; found: C 46.77, H 6.56, N 33.01.

1-Butyl-3-methylimidazolium 2,4-dinitroimidazolate (6c): Colorless oil (90%); ^{1}H NMR: δ = 0.89 (t, J = 7.3 Hz, 3H), 1.32 (sext, J = 7.3 Hz, 2H), 1.81–1.91 (m, 2H), 4.07 (s, 3H), 4.30 (t, J = 7.3 Hz, 2H), 7.52 (t, J = 1.6 Hz, 1H), 7.56 (t, J = 1.5 Hz, 1H), 7.80 (s, 1H), 9.97 ppm (s, 1H); ^{13}C NMR: δ = 13.1, 19.1, 31.8, 36.2, 49.7, 122.1, 123.5, 130.6, 137.3, 147.2, 154.0 ppm; elemental analysis calcd (%) for $C_{11}H_{16}N_6O_4$ (296.3): C 44.59, H 5.44, N 28.36; found: C 44.24, H 5.51, N 28.38.

1-Butyl-3-methylimidazolium 4,5-dinitroimidazolate (6d): Colorless oil (95%); ^{1}H NMR ([D$_6$]DMSO): δ = 0.90 (t, J = 7.3 Hz, 3H), 1.26 (sext, J = 7.4 Hz, 2H), 1.77 (quin, J = 7.3 Hz, 2H), 3.86 (s, 3H), 4.17 (t, J = 7.1 Hz, 2H), 6.96 (s, 1H), 7.71 (t, J = 1.6 Hz, 1H), 7.77 (t, J = 1.6 Hz, 1H), 9.13 ppm (s, 1H); ^{13}C NMR ([D$_6$]DMSO): δ = 13.2, 18.8, 31.4, 35.7, 48.5, 122.3, 123.6, 136.5, 139.4, 140.3 ppm (2C); elemental analysis calcd (%) for $C_{11}H_{16}N_6O_4$ (296.3): C 44.59, H 5.44, N 28.36; found: C 44.21, H 5.44, N 28.45.

1-Butyl-3-methylimidazolium 4,5-dicyanoimidazolate (6e): Colorless oil (98%); ^{1}H NMR: δ = 0.94 (t, J = 7.3 Hz, 3H), 1.35 (sext, J = 7.4 Hz, 2H), 1.81–1.91 (m, 2H), 3.98 (s, 3H), 4.19 (t, J = 7.4 Hz, 2H), 7.40 (s, 1H), 7.41 (s, 1H), 7.46 (s, 1H), 9.26 ppm (s, 1H); ^{13}C NMR: δ = 13.1, 19.2, 31.6, 36.4, 49.8, 116.8, 118.1, 122.3, 123.6, 135.9, 148.8 ppm; elemental analysis calcd (%) for $C_{13}H_{16}N_6$ (256.3): C 60.92, H 6.29, N 32.79; found: C 59.72, H 6.46, N 32.36.

1-Butyl-3-methylimidazolium 4-nitroimidazolate (6f): Colorless oil (96%); ^{1}H NMR: δ = 0.92 (t, J = 7.4 Hz, 3H), 1.32 (sext, J = 7.3 Hz, 2H), 1.81 (quin, J = 7.4 Hz, 2H), 3.94 (s, 3H), 4.17 (t, J = 7.4 Hz, 2H), 7.32–7.34 (m, 3H), 7.36 (s, 1H), 7.96 ppm (s, 1H); ^{13}C NMR: δ = 13.2, 19.3, 31.9, 36.1, 49.6, 121.8, 123.3, 131.9, 137.3 (m, 1C), 146.0, 148.3 ppm; elemental analysis calcd (%) for $C_{11}H_{19}N_5O_3$ (251.3): C 49.06, H 7.11, N 26.01; found: C 49.47, H 7.30, N 26.43.

1-Butyl-3-methylimidazolium tetrazolate (6g): Colorless oil (89%); ^{1}H NMR: δ = 0.89 (t, J = 7.3 Hz, 3H), 1.22–1.34 (m, 2H), 1.73–1.83 (m, 2H), 3.91 (s, 3H), 4.15 (t, J = 7.3 Hz, 2H), 7.39 (s, 1H), 7.44 (s, 1H), 8.39 (s, 1H), 9.72 ppm (s, 1H); ^{13}C NMR: δ = 13.1, 19.1, 31.7, 36.0, 49.4, 121.9, 123.4, 137.1, 149.7 ppm; elemental analysis calcd (%) for $C_9H_{16}N_6$ (208.3): C 51.90, H 7.74, N 40.35; found: C 50.26, H 8.25, N 39.73.

Analysis: Melting points of the isolated salts were determined by using differential scanning calorimetry (MDSC) using a TA Instruments model 2920 Modulated differential scanning calorimeter (New Castle, DE) cooled with a liquid-nitrogen cryostat. The calorimeter was calibrated for temperature and cell constants using indium (m.p. 156.61°C, ΔH° = 28.71 J g^{-1}). Data were collected at constant atmospheric pressure, using samples between 10 and 40 mg in aluminum sample pans sealed by using pin-hole caps. Experiments were performed by heating the samples at a rate of 5°C min^{-1}. The calorimeter was adjusted so that zero heat flow was between 0 and −0.5 mW, and the baseline drift was less than 0.1 mW over the temperature range 0–180°C. An empty sample pan was used as reference.

Thermal decomposition temperatures were measured in the dynamic heating regime using a TGA 2950 TA instrument under argon. Samples between 2 to 10 mg were heated from 40–500°C under constant heating at 5°C min^{-1}.

X-ray crystallographic studies: Samples were recrystallized from methanol by trituration with diethyl ether at 25°C. Single crystals suitable for X-ray analysis were isolated in air, mounted on fibers, and transferred to the goniometer. The crystals were cooled to −100°C with a stream of nitrogen gas and data were collected on a Siemens SMART diffractometer with a charge-coupled device (CCD) area detector, using graphite monochromated $Mo_{K\alpha}$ radiation. The SHELXTL software (version 5) was used for solutions and refinements.[32] Absorption corrections were made with SADABS.[33] Each structure was refined by using full-matrix least-squares methods on F^2.

In each structure, the atoms were readily located; the positions of all non-hydrogen atoms were refined anisotropically. The hydrogen atoms were added in approximated positions and allowed to refine unconstrained in order to obtain proper close-contact interactions. In only one case (**3c**) was disorder observed. The disorder present in the structure was resolved with an occupancy of the two conformations of the disordered methyl group of 70:30. Due to the disorder, the hydrogen atoms of **3c** were added in calculated positions and refined by using a constrained riding model.

CCDC-252733 and 278498–278502 contain the supplementary crystallographic data for salts **4a**, **3c**, **5c**, **5d**, **4e**, and **4f**, respectively. These data can be obtained free of charge from The Cambridge Crystallographic Data Centre via www.ccdc.cam.ac.uk/data_request/cif.

Acknowledgements

This research was supported by the Air Force Office of Scientific Research (grant F49620 03 1 0357).

[1] M. T. Carter, C. L. Hussey, S. K. D. Strubinger, R. A. Osteryoung, *Inorg. Chem.* **1991**, *30*(5), 1149.
[2] T. Welton, *Chem. Rev.* **1999**, *99*, 2071.
[3] J. D. Holbrey, K. R. Seddon, *Clean Prod. Proc.* **1999**, *1*, 223.
[4] P. Wasserscheid, W. Keim, *Angew. Chem.* **2000**, *112*, 3926; *Angew. Chem. Int. Ed.* **2000**, *39*, 3772.
[5] R. Sheldon, *Chem. Commun.* **2001**, 2399.
[6] C. M. Gordon, *Appl. Catal. A* **2001**, *222*, 101.
[7] H. Olivier-Bourbigou, L. Magna, *J. Mol. Catal. A* **2002**, *182–183*, 419.
[8] J. Dupont, R. F. de Souza, P. A. Z. Suarez, *Chem. Rev.* **2002**, *102*, 3667.
[9] K. N. Marsh, J. A. Boxall, R. Lichtenthaler, *Fluid Phase Equilib.* **2004**, *219*, 93.
[10] S. A. Forsyth, J. M. Pringle, D. R. MacFarlane, *Aust. J. Chem.* **2004**, *57*, 113.
[11] T. M. Klapötke, G. Holl, *Green Chem.* **2001**, *3*, G75.
[12] G. Drake, T. Hawkins, A. Brand, L. Hall, M. Mckay, A. Vij, I. Ismail, *Propellants, Explos., Pyrotech.* **2003**, *28*, 174.
[13] Y. X. Ou, B. R. Chen, J. R. Li, S. Dong, J. J. Li, H. P. Jia, *Heterocycles* **1994**, *38*, 1651.
[14] A. R. Katritzky, H. Yang, D. Zhang, K. Kirichenko, J. D. Holbrey, W. M. Reichert, M. Smiglak, R. D. Rogers, *New J. Chem.* **2006**, *30*, 349.
[15] H.-J. Laas, R. Halpaap, F. Richter, J. Kocher, US Pat. App. Pub. 20030204041, **2003**.
[16] W. Ogihara, M. Yoshizawa, H. Ohno, *Chem. Lett.* **2004**, *33*, 1022.
[17] H. Ohno, M. Yoshizawa, W. Ogiwara, H. Ogawa, H. Taguchi, Jpn. Pat. 2004331521, **2004**; [*Chem. Abstr.* **2004**, *141*, 424197].
[18] M. Stearcey, P. L. Pye, J. B. Lee, *Synth. Commun.* **1989**, *19*, 1309.
[19] A. R. Katritzky, S. Singh, K. Kirichenko, J. D. Holbrey, M. Smiglak, W. M. Reichert, R. D. Rogers, *Chem. Commun.* **2005**, 868.
[20] H. Xue, Y. Gao, B. Twamley, J. M. Shreeve, *Inorg. Chem.* **2005**, *44*, 5068.
[21] C. Ye, J. Xiao, B. Twamley, J. M. Shreeve, *Chem. Commun.* **2005**, 2750.
[22] J. D. Holbrey, W. M. Reichert, R. P. Swatloski, G. A. Broker, W. R. Pitner, K. R. Seddon, R. D. Rogers, *Green Chem.* **2002**, *4*, 407.
[23] F. H. Allen, *Acta Crystallogr. Sect. B* **2002**, *58*, 380–388.
[24] P. Duncanson, D. V. Griffiths, J. R. Miller, *Tetrahedron* **1997**, *53*, 13177.
[25] A. Kowalski, *Z. Kristallogr.* **1993**, *208*, 244.
[26] T. Glowiak, Z. Malarski, L. Sobczyk, E. Grech, *J. Mol. Struct.* **1987**, *157*, 329.
[27] V. M. Chernyshev, N. D. Zemlyakov, V. B. Il'in, V. A. Taranushich, *Russ. J. Appl. Chem.* **2000**, *73*, 839; [*Zh. Prikl. Khim. (Russ.)* **2000**, *73(5)*, 791].
[28] T. E. Eagles, M. A. Khan, B. M. Lynch, *Org. Prep. Proced.* **1970**, *2*, 117.
[29] S. S. Novikov, L. I. Khmel'nitskii, O. V. Lebedev, V. V. Sevast'yanova, L. V. Epishina, *Chem. Heterocycl. Compd.* **1970**, *6*, 465.
[30] M. R. Grimmett, S.-T. Hua, K.-C. Chang, S. A. Foley, J. Simpson, *Aust. J. Chem.* **1989**, *42*, 1281.
[31] S. Bulusu, R. Damavarapu, J. R. Autera, R. Behrens, L. M. Minier, J. Villanueva, K. Jayasuriya, T. Axenrod, *J. Phys. Chem.* **1995**, *99*, 5009.
[32] G. M. Sheldrick, SHELXTL, version 5.05, Siemens Analytical X-ray Instruments Inc., **1996**.
[33] G. M. Sheldrick, Program for Semiempirical Absorption Correction of Area Detector Data, University of Göttingen, Göttingen (Germany), **1996**.
[34] J. Sun, M. Forsyth, D. R. MacFarlane, *J. Phys. Chem. B* **1998**, *102*, 8858.
[35] P. Bonhôte, A.-P. Dias, M. Armand, N. Papageorgiou, K. Kalyanasundaram, M. Grätzel, *Inorg. Chem.* **1996**, *35*, 1168.
[36] W. Xu, L.-M. Wang, R. A. Nieman, C. A. Angell, *J. Phys. Chem. B* **2003**, *107*, 11749.
[37] S. J. Kubisen, F. H. Westheimer, *J. Am. Chem. Soc.* **1979**, *101*, 5985.
[38] K. Rousseau, G. C. Farrington, D. Dolphin, *J. Org. Chem.* **1972**, *37*, 3968.
[39] K. Xu, M. S. Ding, T. R. Jow, *J. Electrochem. Soc.* **2001**, *148*, A267.
[40] J. D. Holbrey, K. R. Seddon, *J. Chem. Soc. Dalton Trans.* **1999**, 2133.

Received: July 18, 2005
Revised: January 23, 2006
Published online: April 4, 2006

